CMS Conference Report

October 21, 2006

Physics with tau's in the final states at CMS

Dominique J. Mangeol[1)]

Institut Pluridisciplinaire Hubert Curien, Strasbourg, France

Abstract

On the eve of LHC start-up, the main opportunities offered to CMS to discover and ultimately study new physics with tau's in the final states are presented. From the discovery of the Higgs boson in the Standard Model, of its extension in the MSSM or in non-SUSY alternatives to the measurement of SUSY mass spectrum in $\tilde{q} \to q\tilde{\chi}_2^0 \to q\tau\tilde{\tau}$ cascade decays, this talk reviews the most recent analyses developed in the CMS collaboration for the low luminosity $2 \cdot 10^{33} cm^{-2} s^{-1}$ running phase of the LHC.

Presented at the 9^{th} International Workshop on Tau Lepton Physics, Tau06, September 19-22, 2006, Pisa, Italy

[1)] email: Dominique.J.Mangeol@cern.ch

1 Introduction

This report focuses on the prospect for finding new physics with τ's in the final states. Interests in using τ's include (but are not limited to) their ability to offer a relatively low background environment, a competitive way of probing new physics as well as the possibility to explore new physics regions not accessible otherwise. This report is organized as follows: Section 2 gives an overview of the main Higgs bosons searches in Standard Model and beyond, while Section 3 is dedicated to the investigation of SUSY in di-τ final states.

2 Higgs bosons searches in Standard Model and beyond

2.1 Higgs search in Standard Model

In the Standard Model, the Higgs boson decay to τ pairs is investigated through the vector boson fusion process $qq \rightarrow qqH$ characterized by the emission of the two jets at high rapidity, offering a much reduced background environment compared to the dominant Higgs production process $gg \rightarrow H$. Only events where one τ decays leptonically and the other hadronically are used [1]. The backgrounds surviving the requirement imposed by this topology are $Z/\gamma^{\star} + \mathrm{jets}$, which largely dominates, $W + \mathrm{jets}$ and $t\bar{t}$ productions.

To measure the Higgs boson mass, the di-τ invariant mass distribution is reconstructed using the collinear neutrino approximation. The latter assumes that the τ decay products, including the neutrinos, are emitted along the same direction. Therefore, by using the $E_{\mathrm{T}}^{\mathrm{miss}}$ [2] and its direction in the transverse plane measured with the calorimeters and projecting it along the direction of the τ candidates, it is possible to estimate the momentum of the neutrinos, allowing a precise measurement of the di-τ invariant mass. The di-τ invariant mass for a $135\ \mathrm{GeV}$ Higgs boson together with the main backgrounds is shown in figure 1. The precision of such a measurement relies strongly on the estimation of the $E_{\mathrm{T}}^{\mathrm{miss}}$, which can be monitored by using the knowledge of the position of the Z peak [3].

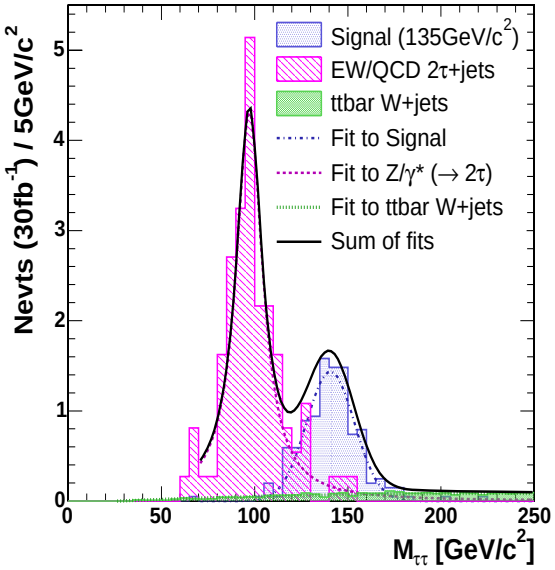

Figure 1: The invariant mass distribution of two reconstructed τ's normalized to the expected number of events at $30\mathrm{fb}^{-1}$.

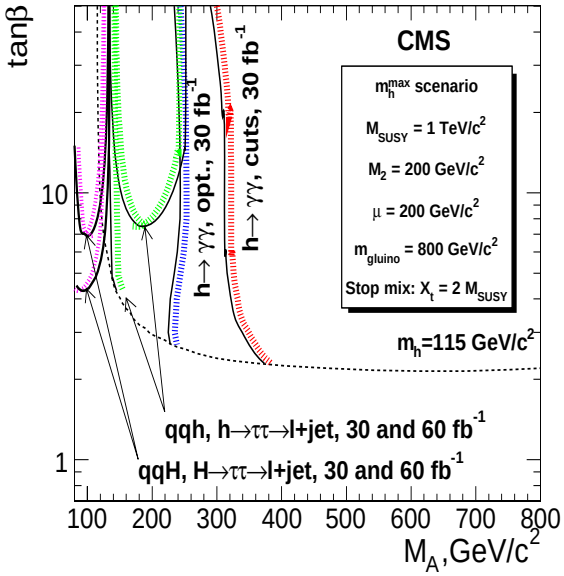

Figure 2: The 5σ discovery region for the light and heavy scalar Higgs bosons, h and H, produced in the vector boson fusion $qq \rightarrow qqh(H)$.

The determination of the signal significance proceeds with the fit of the di-τ invariant mass distribution using information on the shape of the distributions for the signal and the various backgrounds. It is expected that the background distribution shapes will be directly extracted from the data in regions unaffected by a possible signal contribution. The di-τ invariant mass distribution is then parametrized using a combination of the fits to the background distribution shapes scaled to their relative weight in the di-τ invariant mass distribution together with a description of signal distribution depending on the Higgs mass (a Gaussian distribution is used here to describe the signal contribution). The Higgs boson mass hypothesis is then varied until the best agreement with the di-τ

invariant mass distribution is achieved. The number of signal and background events are then evaluated over a $1.5\,\sigma$ window around the nominal Higgs mass.

To achieve a 5σ discovery at least 60fb^{-1} are required for Higgs boson mass hypotheses below 140 GeV. For higher mass, the branching ratio for Higgs boson decaying to di-τ decreases sharply as the di-bosonic Higgs boson decay becomes dominant. This causes the sensitivity of the analysis to the Higgs boson to fade-out.

2.2 MSSM Higgs bosons searches

The results of the previous section can also be interpreted in terms of the MSSM, where the vector boson fusion process leads to the production of light and heavy scalar Higgs bosons. Figure 2 shows the 5σ discovery potential for $qq \to qqH/h$ in $(M_A, \tan\beta)$ plane in the $m_h^{\max}$ scenario for both 30 and 60 fb^{-1}.

An important sign in favour of the discovery of the MSSM Higgs sector at LHC would be the observation of $gg \to b\bar{b}H/A$ which constitutes at large $\tan\beta$ the main process for neutral Higgs boson production. The decay of the neutral Higgs bosons to τ pairs is investigated in four decay modes [4], $\tau{+}\tau \to e{+}\mu; e{+}\tau_{\text{jet}}; \mu{+}\tau_{\text{jet}}; \tau_{\text{jet}}{+}\tau_{\text{jet}}$. The selection of this process is relatively similar for all τ decay modes, however they affect the composition of the remaining backgrounds in different way. Leptonic τ decays will be associated to $Z/\gamma^\star + \text{jets}$ and top-quark production while hadronic τ decays will be responsible for increasing QCD multi-jet background events. Figure 3 shows the 5σ discovery potential for neutral Higgs boson in $(\tan\beta, M_A)$ plane in the maximum mixing scenario with 30 and 60 fb^{-1}. Using the collinear neutrino approximation, as in the previous section, allows, with 60fb^{-1}, to reconstruct the Higgs boson mass with a precision less than 5% (500 GeV Higgs boson mass, $\tan\beta$=30, figure 4) in the $\tau + \tau \to \tau_{\text{jet}} + \tau_{\text{jet}}$ channel, the most challenging one in terms of reconstruction.

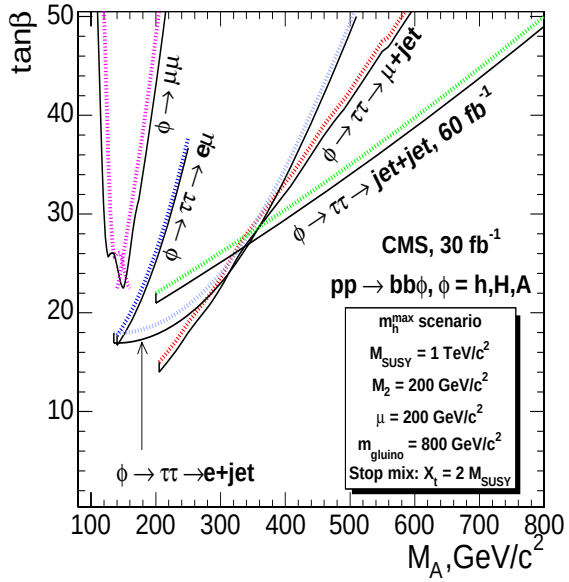

Figure 3: The 5σ discovery regions for the neutral Higgs boson $\phi(\phi = h, H, A)$ produced in association with b quarks in $pp \to b\bar{b}\phi$ with the $\phi \to \mu\mu$ and $\phi \to \tau\tau$ decay modes in the $m_h^{\max}$ scenario.

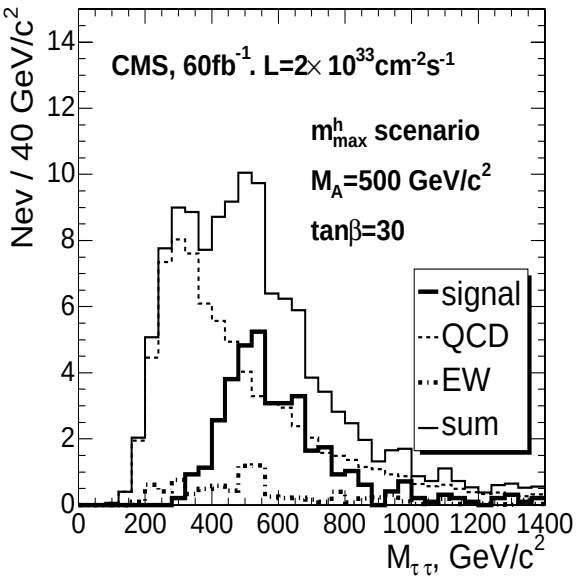

Figure 4: The expected $M_{\tau\tau}$ distribution for a $M_A = 500$ GeV with 60fb^{-1} in the $m_h^{\max}$ scenario.

The charged Higgs boson are also investigated. They are mainly produced at LHC in association with a top quark.

For $m_{H^\pm} < m_t - m_b$ [5], a top-quark may decay to $bH^\pm$. The latter is furthermore predicted to decay almost 100% of the time to $\tau\nu_\tau$. Only hadronic τ decays are used. The search for low mass charged Higgs boson is carried out in $t\bar{t} \to H^\pm bW^\mp\bar{b}$ where the $W^\pm$ boson decays leptonically. The main backgrounds associated to this process are $W + \text{jets}$ and $t\bar{t}$ production.

For $m_{H^\pm} > m_t$ [6], the charged Higgs boson is produced is produced in $gg \to tbH^\pm$. The search proceeds through the reconstruction of the top quark in the fully hadronic channel together with a charged Higgs boson decaying to

$\tau\nu_\tau$, which provides a relatively clean environment. Hadronic τ decay modes are used, allowing the use of the τ polarization properties to effectively discriminate between τ's produced in $W^\pm$ and $H^\pm$ which are produced with opposite polarization states. The backgrounds associated to this channel are W + jets and $t\bar{t}$ production and QCD multi-jets events. Figure 5 shows the 5σ discovery lines for both low and heavy charged Higgs bosons in $(\tan\beta, M_A)$ plane in the maximum mixing scenario obtained with 30fb^{-1}. The mass of the charged Higgs boson could also be extracted from the transverse mass, $m_{\rm T}(\tau_{\rm jet}, E_T^{\rm miss})$, using a Monte Carlo independent method which explicitly takes into account of the τ decays [7].

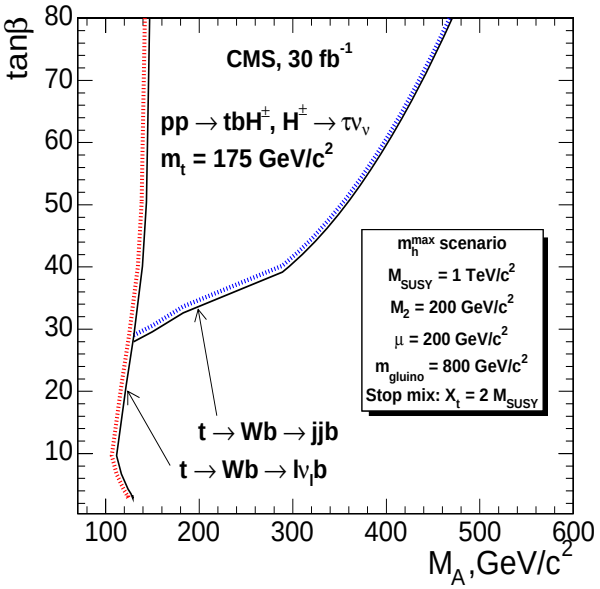

Figure 5: The 5σ discovery regions for the charged Higgs boson decaying to $\tau\nu$ in the $m_h^{\rm max}$ scenario.

2.3 Higgs searches in 5D Randall-Sundrum model

The scalar sector of the 5 dimensional Randall-Sundrum model can be described in terms of four free parameters, ξ, the mixing parameter between the Higgs boson, h and the radion, ϕ, their masses and the vacuum expectation of the radion field, Λ_ϕ. ($m_h = 125$ GeV, $m_\phi = 300$ GeV are used in this analysis).

In this model, Higgs bosons are produced in pairs through the decay of the radion, ϕ. The topology investigated here consists in one Higgs boson decaying to $\tau^\pm\tau^\mp$ while the other decays to $b\bar{b}$. [8] The background associated to this specific signature is dominated by $t\bar{t}$ production. Figure 7 shows the 5σ discovery contour in the (ξ, Λ_ϕ) plane for 30fb^{-1}. The ϕ mass can be accessed by reconstructing both Higgs boson is their respective decay channels as shown in figure 6.

Table 1: Expected number of doubly charged Higgs boson events, NLO cross section with expected statistical and systematic uncertainty of the cross section measurement at 10fb^{-1}, and integrated luminosity needed for exclusion at 95% CL.

$m_\Delta^{\pm\pm}$ (GeV)	200	300	400	500
N_{ev} expected at 10fb^{-1}	26	10	4	2
$\sigma_{\rm NLO} \pm$ stat $\pm$ syst (fb)	$93.9^{+19.3}_{-17.5} \pm 12.2$	$19.6^{+6.6}_{-5.6} \pm 2.5$	$5.9^{+3.4}_{-2.5} \pm 0.8$	$2.2^{+1.9}_{-1.3} \pm 0.3$
Luminosity for 95% CL exclusion,fb^{-1}	1.3	3.0	7.7	16.8

2.4 Doubly charged Higgs boson in the Little Higgs Model

In the Little Higgs model, the doubly charged Higgs boson, $\Delta^{\pm\pm}$, can be produced either through vector boson fusion or in pair in the Drell-Yann process. The doubly charged Higgs boson is expected to decay equally to $\mu^\pm\mu^\pm, \mu^\pm\tau^\pm, \tau^\pm\tau^\pm$. This analysis focuses on $\Delta^{\pm\pm}$ pair production in the Drell-Yann process with up to three τ's in the final states. The requirement of having four objects (either muons or τ's) allows a background free environment [9]. For $m_{\Delta^{\pm\pm}} = 200$ GeV 26 events are expected, while only 2 survives the selection for $m_{\Delta^{\pm\pm}} = 500$ GeV (table 1).

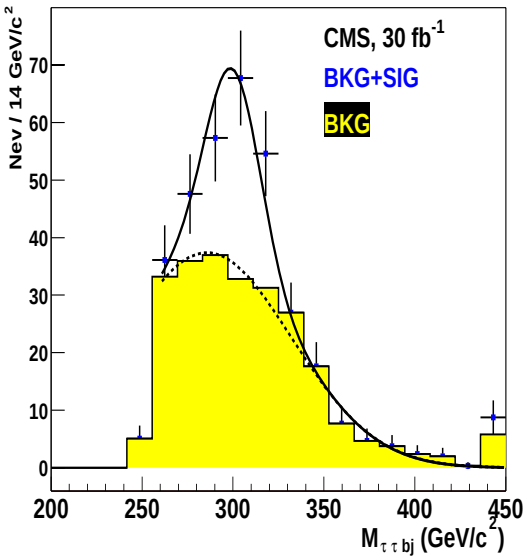

Figure 6: The $M_{\tau\tau bj}$ distribution for the background (full gray histogram) and the signal of $\phi \rightarrow hh \rightarrow \tau\tau b\bar{b}$ plus background (black dots) after selection with 30fb^{-1}.

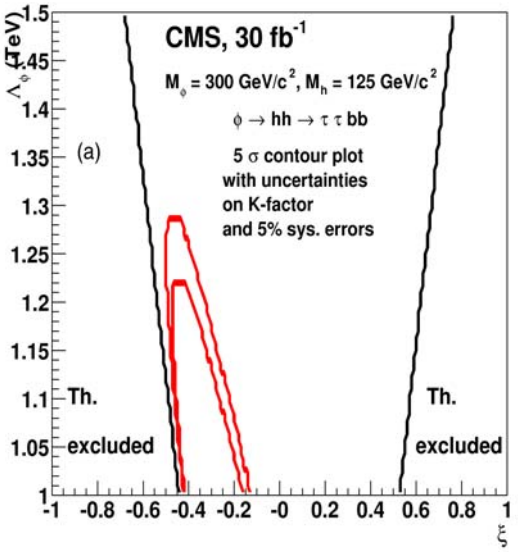

Figure 7: The 5σ discovery contours for the $\phi \rightarrow hh \rightarrow \tau\tau b\bar{b}$ with 30fb^{-1}. The two contours corresponds to the variation of the background NLO cross section due to the scale uncertainty.

3 Search for SUSY in di-τ final states

In proton-proton collision, SUSY is mainly produced through $\tilde{q}$ and $\tilde{g}$ pair production. The $\tilde{q}$ and $\tilde{g}$ eventually decay to the lightest supersymmetric particle (LSP) through cascade decays of variable "length". In R-parity conserved model, like the one investigated here, the LSP is weakly interacting and escape detection, forbidding a direct measurement of the mass of the sparticles. The cascade decay $\tilde{q} \rightarrow q\tilde{\chi}_2^0 \rightarrow q\tau\tilde{\tau}$ which is investigated in the mSUGRA context [10] is of great interest. At low $\tan\beta$, the branching fraction for $\tilde{\chi}_2^0 \rightarrow \tau\tilde{\tau}$ is of the same order as for the other slepton production while at large $\tan\beta$ it becomes 96%, hence becoming the only way to probe this sector of SUSY.

3.1 Inclusive search for SUSY in di-τ final states

The inclusive search for SUSY in di-τ final states is initiated by requiring a large $E_{\mathrm{T}}^{\mathrm{miss}}$ (because of the LSP), two very energetic jets (since the cascades are produced in pairs) and at least two τ's decaying hadronically [11]. The main backgrounds associated to this process are QCD multi-jet events, $t\bar{t}$ production and $W+\mathrm{jets}$. Figure 8 and 9 show the 5σ discovery contours over the mSUGRA $(m_0, m_{1/2})$ plane ($A_0 = 0$ and $\mu > 0$) for several integrated luminosities between 0.1 and 10fb^{-1} for $\tan\beta$=10 and $\tan\beta$=35, respectively. It must be noted that $\tilde{\chi}_2^0$ cascade decays occur only for low m_0 values and the sensitivity to SUSY for large m_0 is caused by the presence of Higgs bosons decaying to τ's.

3.2 Measurement of SUSY mass spectrum in $\tilde{q} \rightarrow q\tilde{\chi}_2^0 \rightarrow q\tau\tilde{\tau}$ cascade

The cascade decay chain $\tilde{q} \rightarrow q\tilde{\chi}_2^0 \rightarrow q\tau\tilde{\tau} \rightarrow q\tau\tau\tilde{\chi}_1^0$ allows the use of the kinematic edge technique to extract the mass of the sparticles [12]. This technique takes advantage of the three two-body decays present in the cascade to build four relations between the four sparticles masses and the end-points of the invariant mass distributions obtained by combining the quark-jet and the two τ observed in the final states. The absence of detection of the neutrinos produced in the decay of the τ's largely complicates the reconstruction and the extraction of the mass spectrum.

The end-points are obtained from the fits of the various invariant mass distributions taking into account the large combinatorial background due to multiple τ and jet associations as well as the remaining physics backgrounds

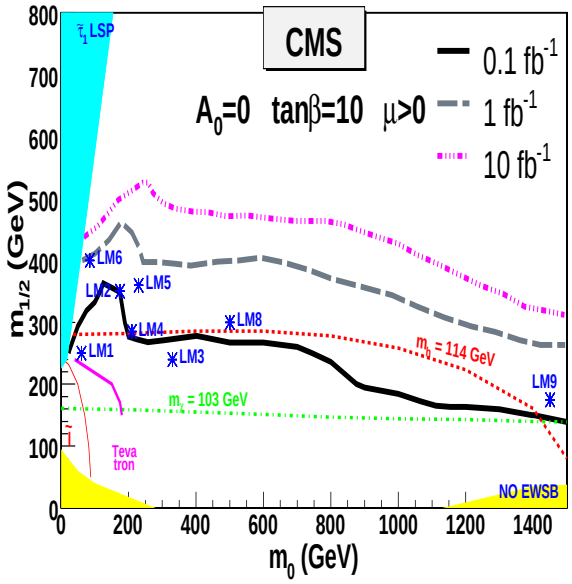

Figure 8: 5σ discovery contours for integrated luminosities between 0.1 and 10 fb^{-1} at $\tan\beta = 10$ obtained by taking into account of the systematic uncertainties on the background in the significance.

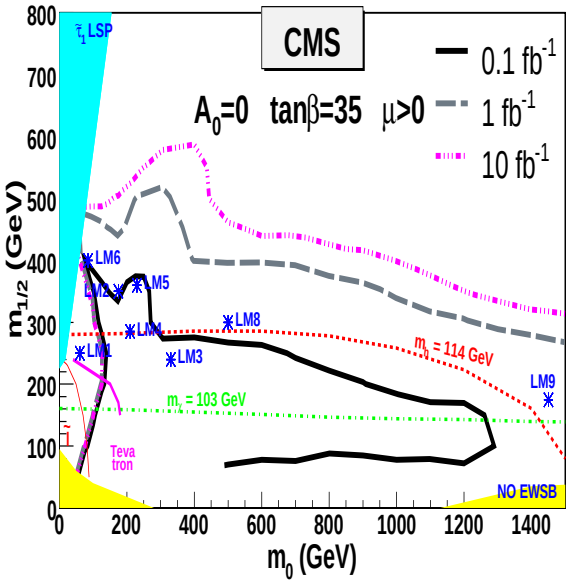

Figure 9: 5σ discovery contours for integrated luminosities between 0.1 and 10 fb^{-1} at $\tan\beta = 35$ obtained by taking into account of the systematic uncertainties on the background in the significance.

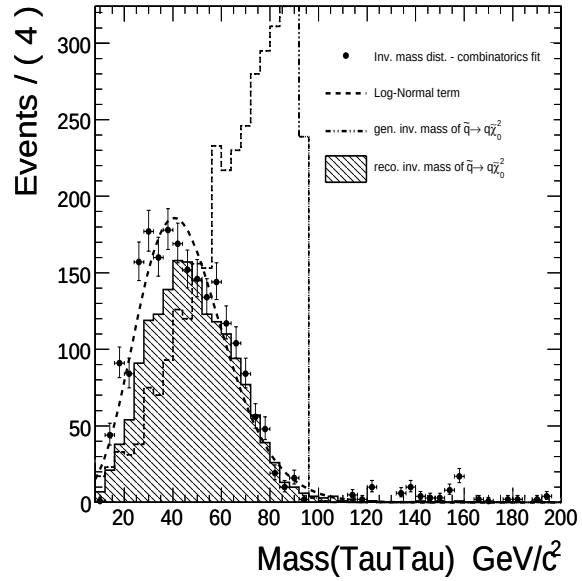

Figure 10: Di-τ invariant mass distribution of the signal obtained after subtracting the combinatorial fit together with the log-normal term used in the invariant mass fit.

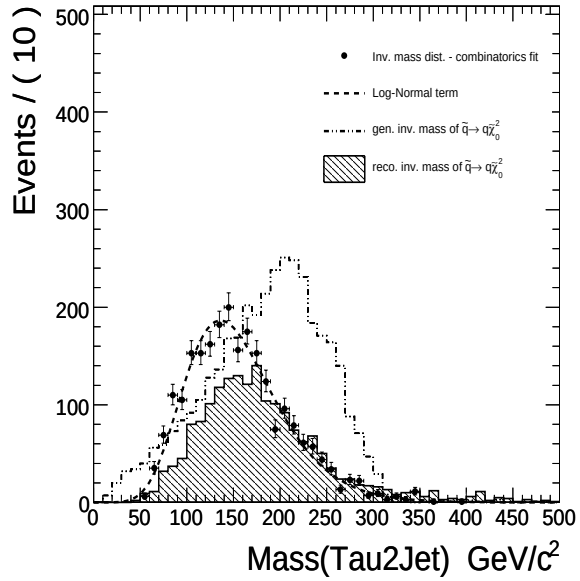

Figure 11: $m(\tau_1 q)$ invariant mass distribution of the signal obtained after subtracting the combinatorial fit together with the log-normal term used in the invariant mass fit.

(see [11] for details). Examples of invariant mass distributions at the LM2 test point ($m_0 = 185$ GeV, $m_{1/2} = 350$ GeV, $\tan\beta = 35$, $A_0 = 0$ and $\mu > 0$) are shown in figure 10 and 11 after combinatorial background has been removed. The sparticles masses obtained from the end-points with 40 fb^{-1} are shown together with their theoretical values for the LM2 test point in table 2. They are in good agreement with their theoretical counterparts.

Table 2: Sparticle masses measured with end-point method together with theoretical value at the LM2 test point. The first uncertainties are statistical, the second systematic.

	measured (GeV)	theory (GeV)
$M(\tilde{\chi}_1^0)$	$147 \pm 23 \pm 19$	138.2
$M(\tilde{\chi}_2^0)$	$265 \pm 10 \pm 25$	265.5
$M(\tilde{\tau})$	$165 \pm 10 \pm 20$	153.9
$M(\tilde{q})$	$763 \pm 33 \pm 58$	753-783 (light $\tilde{q}$)

4 Conclusions

In this conference report, the most recent analyses using τ's in the final states developed in the CMS collaboration in view of the low luminosity $2 \cdot 10^{33} cm^{-2} s^{-1}$ running phase of the LHC have been reviewed. These event topologies allow a very effective exploration of new physics. More particularly, low mass charged Higgs boson, high $\tan\beta$ SUSY cascade decays which can only be accessed through τ's final states. Even if somewhat more challenging, Higgs mass measurement and SUSY mass spectrum can also be measured with good precision.

5 Acknowledgments

The author would like to thank Sasha Nikitenko and Roberto Tenchini for the careful reading of the conference note.

References

[1] C. Foudas et al. **CMS Note 2006/088**.

[2] Haifeng Pi et al. **CMS Note 2006/035**.

[3] A. Kalinowski et al. **CMS Note 2006/074**.

[4] S. Lehti et al. **CMS Note 2006/101**; R. Kinnunen et al. **CMS Note 2006/075**; A. Kalinowski et al. **CMS Note 2006/105**; S. Gennai et al. **CMS Note 2006/126**.

[5] M. Baarmand et al. **CMS Note 2006/056**.

[6] R. Kinnunen et al. **CMS Note 2006/100**.

[7] S. R. Slabospitsky **CMS Note 2002/010**.

[8] D. Dominici et al. **CMS Note 2005/071**.

[9] CMS Physics TDR, Volume II: Physics Performance **CERN/LHCC 2006-021**

[10] H. P. Nilles, **Phys. Reports, 110 (1984) 1**; P. Nath et al. *Applied N=1 Supergravity* **World Scientific Singapore, 1984**; S. P. Martin *Perspectives on supersymmetry* **World Scientific Singapore, 1998**.

[11] D. J. Mangeol et al. **CMS Note 2006/096**.

[12] B. K. Gjelsten et al., **JHEP 0412:003,2004**.